BUDAPEST UNIVERSITY OF TECHNOLOGY AND ECONOMICS

Faculty of Electrical Engineering and Informatics

Department of Networked Systems and Services
Mobile Communications and Quantum Technologies Laboratory

CHANNEL EQUALIZATION AND MOBILITY MANAGEMENT METHODS IN NEW GENERATION MOBILE COMMUNICATION SYSTEMS

Ph. D. Thesis booklet of

Ádám Knapp

Scientific supervisor:

László Pap, Member of MTA

Budapest, 2019

1 Introduction

The wireless and mobile communication have been significantly evolved during the last decades. This evolution have been driven by the increasing demands for higher throughput by human users and their changed behaviour. In addition, new group of end users appeared with specific requirements in the last couple of years, namely industry and machines. Internet of Things (IoT), Industrial IoT and Industry 4.0 are such, but similar technologies that focus on these usage domains. The specific requirements of the machines and the industry became determinative in the telecommunication area. Therefore the research and standardization activities take into consideration these requirements, and the next generation networks are planned and prepared to satisfy them more efficiently than nowadays. The requirements of machine-to-machine (M2M) or machine type communication (MTC) in other words include high and constant data throughput, low latency, reliable and robust transmission, high availability, high energy efficiency and low power operations. These are often contradictory from practical aspects, thus specialized communication solutions are developed and started to spread in the world beside the traditional cellular mobile networks.

Low-Power Wide Area Networks (LPWAN) technologies usually handle fixed devices that are often operated from batteries, mobile terminals are not considered. In the related doctoral thesis I propose a system that is similar to LPWAN, however, it addresses different use cases where terminals are able to move, for example, factory logistic vehicles, even with high speeds, like unmanned aerial vehicles (UAV). Such use cases can be found for fifth generation mobile communication networks (5G) as well. One of the key domains of 5G is M2M communication, however, the complexity, the energy efficiency and the price of receivers makes 5G an uncompetitive technology on the field of LPWAN.

Spread Spectrum (SS) and Closed-Loop Power Control (CLPC) techniques are well-known from decades. SS communication is widely spread, standardized in many ways, and different forms are applied in vast of communication devices. On the one hand, the communication are based on Direct-Sequence Spread Spectrum (DSSS) technique in IEEE 802.11b standards, as the original Wi-Fi system; in IEEE 802.15.4 standard, which is the physical layer for ZigBee; in Code Division Multiple Access (CDMA) channel access method and in different Global Navigation Satellite Systems (GNSS) like GPS, GLONASS and Galileo. On the other hand, Adaptive Frequency-hopping spread spectrum (AFH) is applied in Bluetooth, which is a variant of Frequency-Hopping Spread Spectrum (FHSS) technique. Finally, Chirp Spread Spectrum (CSS) is important part of IEEE 802.15.4a standard as a supported physical layer in Low-Rate Wireless Personal Area Networks (LR-WPAN) and of LoRaWAN (Long Range Wide Area Network), which is an emerging communications technology for LPWAN as well. The reasons can be found among the advantages of CSS, which include high robustness against channel noise, interference and jamming. Furthermore, the resistance capability against the Doppler effect makes CSS a very good candidate in such mobile communication environment, where support for terminals moving with high speeds and at long ranges is necessary.

The importance of closed-loop power control and channel equalization has been shown by the traditional cellular mobile communication networks. The former handles the so-called near-far problem, which is a quite common issue in mobile networks, while the latter compensates the effect of random fluctuation (fading) appearing in the radio channel. CLPC is part of the operation in 2G GSM as well, however, its significance improved in 3G CDMA-based cellular systems, which utilize CLPC to mitigate in-system interference. The closed-loop power control is also important in fourth generation systems (like 3GPP LTE and its advanced versions) in connection with Multiple Input Multiple Output (MIMO) technologies. It has central role in new directions of mobile communication systems, such as cognitive radio systems. This is motivated by the recent standardization trends towards permitting different heterogeneous communication systems to coexist and share a common wireless channel (e.g. unlicensed spectrum, opportunistic and dynamic spectrum access, spectrum underlay or overlay, etc.). CLPC and channel equalization has been further evolved in the 3GPP New Radio (NR), that is a fifth generation mobile cellular network, by using reference and synchronization signals, i.e. training signals for CLPC and channel equalization, in a more sophisticated way.

Besides handling the prior problems for efficient and reliable communication, the issues related to handovers have to be managed in public cellular networks for higher user experience and for better system performance. One consequence of such networks' evolution is that the cell sizes are shrinking, while higher user throughput has been achieved. For example the typical cell radius is around several tens of kilometres in 2G GSM, whilst most of 4G LTE cells have ca. 500 m. Furthermore, other deployment scenarios appeared in the recent standards that take into account the coexistence of much smaller cells under the traditional macro cells. In such heterogeneous, two-tier network the other layer beside the macro cells is collectively called small cells. These can be micro, pico or femto cells depending on their coverage area and feature sets. The latest one is the so-called Home eNodeB in 3GPP terminology that defines a base station deployed by users and not the operator. It is designed to serve a flat or small office and connect to the Mobile Network Operator's network via public Internet connection. Furthermore, outdoor use cases are foreseen as well in that the small cells behave similarly to Wi-Fi access points and provide improved local service. These concepts are further improved in 5G networks. Nevertheless, one of the main challenges is the handover procedure and decision mechanism in this kind of two-tier network.

1.1 Research Objectives

The dissertation summarizes all my research results from the recent years. By investigating the channel equalization mechanism, formulas are derived that give good estimation of bit-error and symbol-error rates, as well as they are applicable in practice. Similarly, spread spectrum based radio systems are analysed, where results related to correlation peak detection are determined. The outcome of these investigation allowed to construct a novel communication system that combines pulse position modulation with chirp spread spectrum transmission schema. Finally, a practical handover decision algorithm is provided to utilize the small cells even more in LTE/LTE-A network.

The goal of the theorems related to measurement based feedback channel equalization is to present a unified analytical method for the accurate error rate analysis of coherent Binary Phase Shift Keying (BPSK) and orthogonal noncoherent Binary Frequency Shift Keying (BFSK) modulations in wireless communication systems with fast closed-loop power control mechanisms subjected to general fading and using a measuring based channel estimation in a separated noisy channel. The main contributions are new exact expressions for error rates of coherent BPSK and orthogonal noncoherent BFSK modulations in different fading environments (including Rayleigh, Nakagami, and Rician fading) and subjected to a non-exact channel transmission parameter measured in a noisy pilot channel. The results of this dissertation can be used to compare the performance of a coherent BPSK or orthogonal noncoherent BFSK wireless network that has a fast closed-loop power control system and uses diversity combining algorithms to parallel solve the near-far problem and channel equalization.

Then, the investigations related to correlation peak detection enables to construct a more precise synchronization system for spread spectrum based communication techniques, as well as to utilize this improved synchronization for network services such as localization. A new correlator is proposed namely the sliding-and-tracking correlator that is based on the cooperation of two correlators. Mathematical model is established to investigate and compare the wrong decision probability of the sliding-and-tracking correlator against the traditional sliding correlator. Furthermore, I also developed a communication system that partially applies these results and partially uses the prior CLPC mechanism. The key feature of the scheme is that it provides simultaneous transmission for multiple mobile terminals using a new communication method. The method combines the pulse position modulation with the chirp spread spectrum technique. This transmission scheme is able to work by itself as LPWAN.

In the last section, I focus on the handover decision algorithms of the two-tier LTE/LTE-A network. Furthermore, I propose a new decision procedure that takes into account several parameters, like the speed of the UEs and the actual load of neighbouring cells. The handover decision algorithm and the related results can support the standardization activities of future mobile cellular network, particularly the New Radio. It is a candidate fifth generation standard for global usage advocated by many communication companies worldwide under the aegis of the 3rd Generation Partnership Project (3GPP).

1.2 Research Methodology

My research topics are based on different system models that are described in the dissertation in details. Therefore, the three thesis group that are presented in this leaflet reflect this classification as well.

In my first thesis group (*Thesis group I.*), channel equalization related researches are presented. A novel amplitude equalization method is described, which feedbacks the results of the measurement channel transmitting the training signal to the receiver, and the data carrying signal is equalized in the transmitter side. The first thesis introduces the general bit-error rate formula for the measurement based feedback channel equalization that contains the channel's

fading function as a general parameter. Then, the next thesis provides exact calculations for popular fading model types, namely Rayleigh, Rice and Nakagami fadings. Furthermore, the method was further improved by taking into account the maximum transmission power as an input parameter of the expressions. The related formulas are described in the third and forth theses. Thus, these expressions reflect even more practical aspects. The theoretical results are validated against simulation results.

The fifth thesis takes into consideration the phase shifting characteristic of the channel and gives exact Bit Error Rate (BER) expressions for BPSK and QPSK modulations. These investigations led to an optimization problem. Its numerical solution is introduced according to the LTE/LTE-A system.

My second thesis group (*Thesis group II.*) is about analysing spread spectrum based systems. A novel method is described and analysed for correlation peak detection as the first thesis in this thesis group. Then, the second thesis introduces exact bit error rate calculations for the detection method. Using these results, new multi-user schemes are defined for chirp spread spectrum based communication systems in the third thesis. The forth thesis contains the BER related performance investigations of the proposed system.

The third thesis group (*Thesis group III.*) consists of one thesis. I propose a novel hybrid handover decision algorithm that uses the velocity of the user equipment, the load and the RSSI of the candidate cells, as well as their access mode. So, it provides load balancing in the network. The algorithm is implemented in a C++ based LTE simulation software that was developed at the department. The performance related results, like overall throughput, average user latency and number of handovers are compared to the legacy handover decision algorithm.

2 New scientific contributions

This section introduces the new scientific results in the form of theses. Each thesis consists of several theorems, lemmas, corollaries or definitions that are detailed in the dissertation.

2.1 Channel equalization

The corresponding chapter in the dissertation introduces the channel equalization related theorems. First, the measurement based feedback channel equalization is discussed. Bit error rates can be calculated using the proposed exact formulas, while taking into account the SNR values of the measurement and the normal, data communication channels. Then, symbol error rate expressions are presented that are related to the estimation error of the signal's phase component.

The theorems are collected into five theses that make the first thesis group.

2.1.1 Measurement based feedback channel equalization

In the last two decades intensive investigations of wireless systems with closed-loop power control and channel equalization have been carried out. This area in different contexts but always raised in every generation of mobile communication systems. The CLPC solves the so-called near-far problem primarily, however, the channel equalization compensates the effect of random fluctuation (fading) appearing in the radio channel. Traditionally, the prior problem is used to be solved with a high delay closed-loop power control system, while solution of the latter one requires diversity techniques [1]. The closed-loop power control had an important role in the early mobile technologies (i.e. NMT and GSM), however, its significance increased when the third generation CDMA systems were introduced. These systems require power control for the in-system interference coordination to provide reliable and fair communication. This topic remained in focus since then, numerous papers were published in the recent years. The closed-loop power control is also important in fourth generation systems (Long Term Evolution and its advanced versions) in connection with MIMO technologies as well as in 5G that enables the usage of higher order and more advanced multi-antenna techniques including 128 or even more antenna elements [2]-[4].

THESIS I.1. [J1] *I presented an analytical calculation method to determine the bit error rate for such transmission scheme that applies measurement based feedback channel equalization. The method takes into consideration the estimation error of the signal's amplitude that originates from general fading channel.*

The related theorems from the dissertation are the following.

- **Theorem 2.1.** The following analytical expression determines the average bit error probability in the *theoretical* measurement based feedback channel equalization model assum-

ing coherent binary transmission and taking into account the general fading model:

$$P_b(\gamma_s) = \frac{1}{\pi} \int_0^{\infty} \int_0^{\infty} \int_0^{\frac{\pi}{2}} \exp\left(-\frac{\gamma_s x}{y\cos^2(\theta)}\right) \gamma_0 \exp\left(-\gamma_0 (x+y)\right) I_0\left(2\gamma_0\sqrt{xy}\right) f_X(x)\, d\theta dx dy, \tag{1}$$

where $I_0(.)$ is the modified Bessel function of the first kind and zeroth order, $f_X(x)$ is the PDF of the general fading channel gain, γ_0 is the SNR of the measurement channel and γ_s is the SNR of the communication channel.

- **Theorem 2.9.** The average bit error probability function is given by the following formula in the *theoretical* measurement based feedback channel equalization model supposing noncoherent binary transmission and taking into account the general fading model:

$$P_b(\gamma_s) = \frac{1}{2} \int_0^{\infty} \int_0^{\infty} \exp\left(-\frac{\gamma_s x}{2y}\right) f_{XY}(x,y)\, dx dy, \tag{2}$$

where

$$f_{XY}(x,y) = f_{Y|X}(y|x)\, f_X(x).$$

THESIS I.2. [J1] *I derived exact formulas to calculate the BER of measurement based feedback channel equalization for Rayleigh, Rice and Nakagami fading models, as well as assuming that the transmission power can be infinite.*

The related theorems from the dissertation are listed below.

- **Theorem 2.3.** The average bit error probability function is given by the following expression in the *theoretical* measurement based feedback channel equalization model assuming coherent binary transmission and Rayleigh fading model:

$$P_b(\gamma_s) = \frac{\gamma_0}{\pi} \int_0^{\frac{\pi}{2}} \int_0^{\infty} \frac{1}{1+\gamma_0+\frac{\gamma_s}{y\cos^2(\theta)}} \exp\left(-\gamma_0 y \frac{1+\frac{\gamma_s}{y\cos^2(\theta)}}{1+\gamma_0+\frac{\gamma_s}{y\cos^2(\theta)}}\right) dy d\theta. \tag{3}$$

- **Theorem 2.5.** The average bit error probability function is given by the following expression in the *theoretical* measurement based feedback channel equalization model assuming coherent binary transmission and Rician fading model:

$$P_b(\gamma_s) = \frac{\gamma_0}{\pi} \int_0^{\frac{\pi}{2}} \sum_{l=0}^{\infty} \frac{k^l (1+k)^l}{l!} \int_0^{\infty} {}_1F_1\left(l+1, 1; \frac{\gamma_0^2 y}{(1+k)+\gamma_0+\frac{\gamma_s}{y\cos^2(\theta)}}\right) \frac{\exp(-\gamma_0 y)\exp(-k)}{\left((1+k)+\gamma_0+\frac{\gamma_s}{y\cos^2(\theta)}\right)^{l+1}} dy d\theta, \tag{4}$$

where k is the parameter of the Rician distribution and ${}_1F_1(.,.;.)$ is the confluent hypergeometric function.

- **Theorem 2.7.** The following exact formula determines the average bit error probability in the *theoretical* measurement based feedback channel equalization model supposing coherent binary transmission and Nakagami fading model:

$$P_b(\gamma_s) = \frac{\gamma_0 m^m}{\pi} \int_0^{\frac{\pi}{2}} \int_0^{\infty} \frac{\exp(-\gamma_0 y)}{\left(m+\gamma_0+\frac{\gamma_s}{y\cos^2(\theta)}\right)^m} {}_1F_1\left(m,1;\frac{\gamma_0^2 y}{m+\gamma_0+\frac{\gamma_s}{y\cos^2(\theta)}}\right) dy d\theta, \quad (5)$$

where m is the parameter of the Nakagami distribution.

- **Theorem 2.11.** The average bit error probability function is given by the following expression in the *theoretical* measurement based feedback channel equalization model assuming noncoherent binary transmission and Rayleigh fading model:

$$P_b(\gamma_s) = \frac{\gamma_0}{2} \int_0^{\infty} \frac{1}{1+\gamma_0+\frac{\gamma_s}{2y}} \exp\left(-\gamma_0 y \frac{1+\frac{\gamma_s}{2y}}{1+\gamma_0+\frac{\gamma_s}{2y}}\right) dy. \quad (6)$$

- **Theorem 2.13.** The following exact formula determines the average bit error probability in the *theoretical* measurement based feedback channel equalization model supposing coherent binary transmission and Rician fading model:

$$P_b(\gamma_s) = \frac{\gamma_0}{2} \sum_{l=0}^{\infty} \frac{k^l (1+k)^l}{l!} \int_0^{\infty} \frac{\exp(-\gamma_0 y)\exp(-k)}{\left((1+k)+\gamma_0+\frac{\gamma_s}{2y}\right)^{l+1}} {}_1F_1\left(l+1,1;\frac{\gamma_0^2 y}{(1+k)+\gamma_0+\frac{\gamma_s}{2y}}\right) dy. \quad (7)$$

- **Theorem 2.15.** The average bit error probability is given by the following expression in the *theoretical* measurement based feedback channel equalization model supposing noncoherent binary transmission and Nakagami fading model:

$$P_b(\gamma_s) = \frac{\gamma_0 m^m}{2} \int_0^{\infty} \frac{\exp(-\gamma_0 y)}{\left(m+\gamma_0+\frac{\gamma_s}{2h(y)}\right)^m} {}_1F_1\left(m,1;\frac{\gamma_0^2 y}{m+\gamma_0+\frac{\gamma_s}{2h(y)}}\right) dy. \quad (8)$$

THESIS I.3. [J1] *I extended the system model and the calculations to take into account the maximum transmission power as a constraint.*

The related theorems from the dissertation are the following.

- **Theorem 2.2.** The following analytical expression determines the average bit error probability in the *practical* measurement based feedback channel equalization model assuming coherent binary transmission and taking into account the general fading model:

$$P_b(\gamma_s) = \frac{1}{\pi} \int_0^{\infty} \int_0^{\infty} \int_0^{\frac{\pi}{2}} \exp\left(-\frac{\gamma_s x}{y' \cos^2(\theta)}\right) f_{XY'}(x,y')\, d\theta dx dy', \tag{9}$$

  where y' and $f_{XY'}(x,y')$ is given as follows:

$$h(y) = y' = \begin{cases} c & \text{if } y \leq c \\ y & \text{if } y > c \end{cases}$$

  and

$$f_{XY'}(x,y') = \begin{cases} A(x)\,\delta(y'-c) f_X(x) & \text{if } y' = c \\ f_{Y|X}(y'|x)\, f_X(x) & \text{if } y' > c \end{cases},$$

  where

$$A(x) = \int_0^{c} f_{Y|X}(y|x)\, dy.$$

- **Theorem 2.10.** The average bit error probability function is given by the following expression in the *practical* measurement based feedback channel equalization model supposing noncoherent binary transmission and taking into account the general fading model:

$$P_b(\gamma_s) = \frac{1}{2} \int_0^{\infty} \int_0^{\infty} \exp\left(-\frac{\gamma_s x}{2h(y)}\right) f_{XY'}(x,y')\, dx dy', \tag{10}$$

  where y' and $f_{XY'}(x,y')$ are the same as before.

THESIS I.4. [J1] *I transformed the exact expressions according to this new system model, and determined the BER of measurement based feedback channel equalization for Rayleigh, Rice and Nakagami fading models.*

The related theorems from the dissertation are listed below.

- **Theorem 2.4.** The average bit error probability function is given by the following expression in the *practical* measurement based feedback channel equalization model assuming coherent binary transmission and Rayleigh fading model:

$$P_b(\gamma_s) = \frac{\gamma_0}{\pi} \int_0^{\frac{\pi}{2}} \int_0^{\infty} \frac{1}{1+\gamma_0+\frac{\gamma_s}{h(y)\cos^2(\theta)}} \exp\left(-\gamma_0 y \frac{1+\frac{\gamma_s}{h(y)\cos^2(\theta)}}{1+\gamma_0+\frac{\gamma_s}{h(y)\cos^2(\theta)}}\right) dy d\theta, \quad (11)$$

where the integral by y should be calculated in two intervals: $\{[0,c]\,;\, h(y)=c\}$ and $\{(c,\infty)\,;\, h(y)=y\}$.

- **Theorem 2.6.** The average bit error probability function is given by the following expression in the *practical* measurement based feedback channel equalization model assuming coherent binary transmission and Rician fading model:

$$P_b(\gamma_s) = \frac{\gamma_0}{\pi} \int_0^{\frac{\pi}{2}} \sum_{l=0}^{\infty} \frac{k^l (1+k)^l}{l!} \int_0^{\infty} {}_1F_1\left(l+1,1;\frac{\gamma_0^2 y}{(1+k)+\gamma_0+\frac{\gamma_s}{h(y)\cos^2(\theta)}}\right) \frac{\exp(-\gamma_0 y)\exp(-k)}{\left((1+k)+\gamma_0+\frac{\gamma_s}{h(y)\cos^2(\theta)}\right)^{l+1}} dy d\theta. \quad (12)$$

- **Theorem 2.8.** The following exact formula determines the average bit error probability in the *practical* measurement based feedback channel equalization model supposing coherent binary transmission and Nakagami fading model:

$$P_b(\gamma_s) = \frac{\gamma_0 m^m}{\pi} \int_0^{\frac{\pi}{2}} \int_0^{\infty} \frac{\exp(-\gamma_0 y)}{\left(m+\gamma_0+\frac{\gamma_s}{h(y)\cos^2(\theta)}\right)^m} {}_1F_1\left(m,1;\frac{\gamma_0^2 y}{m+\gamma_0+\frac{\gamma_s}{h(y)\cos^2(\theta)}}\right) dy d\theta. \quad (13)$$

- **Theorem 2.12.** The average bit error probability function is given by the following expression in the *practical* measurement based feedback channel equalization model supposing noncoherent binary transmission and Rayleigh fading model:

$$P_b(\gamma_s) = \frac{\gamma_0}{2} \int_0^{\infty} \frac{1}{1+\gamma_0+\frac{\gamma_s}{2h(y)}} \exp\left(-\gamma_0 y \frac{1+\frac{\gamma_s}{2h(y)}}{1+\gamma_0+\frac{\gamma_s}{2h(y)}}\right) dy. \quad (14)$$

- **Theorem 2.14.** The following exact formula determines the average bit error probability in the *practical* measurement based feedback channel equalization model assuming noncoherent binary transmission and Rician fading model:

$$P_b(\gamma_s) = \frac{\gamma_0}{2} \sum_{l=0}^{\infty} \frac{k^l (1+k)^l}{l!} \int_0^{\infty} \frac{\exp(-\gamma_0 y) \exp(-k)}{\left((1+k)+\gamma_0+\frac{\gamma_s}{2h(y)}\right)^{l+1}} {}_1F_1\left(l+1,1;\frac{\gamma_0^2 y}{(1+k)+\gamma_0+\frac{\gamma_s}{2h(y)}}\right) dy. \tag{15}$$

- **Theorem 2.16.** The average bit error probability is given by the following expression in the *practical* measurement based feedback channel equalization model supposing noncoherent binary transmission and Nakagami fading model:

$$P_b(\gamma_s) = \frac{\gamma_0 m^m}{2} \int_0^{\infty} \frac{\exp(-\gamma_0 y)}{\left(m+\gamma_0+\frac{\gamma_s}{2h(y)}\right)^m} {}_1F_1\left(m,1;\frac{\gamma_0^2 y}{m+\gamma_0+\frac{\gamma_s}{2h(y)}}\right) dy. \tag{16}$$

- **Theorem 2.17.** The average SNR change is given by the following formula assuming the *practical* measurement based feedback channel equalization model and Rayleigh fading as channel model:

$$\mathbb{E}\left[\frac{\mathrm{SNR}}{\gamma_s}\right] = \int_0^{\infty} \frac{1}{h(y)} \frac{\gamma_0}{1+\gamma_0} \exp\left(-\frac{\gamma_0}{1+\gamma_0} y\right) dy. \tag{17}$$

- **Theorem 2.18.** The average SNR change is described by the following expression supposing the *practical* measurement based feedback channel equalization model and Rician fading as channel model:

$$\mathbb{E}\left[\frac{\mathrm{SNR}}{\gamma_s}\right] = \int_0^{\infty} \sum_{l=0}^{\infty} \frac{k^l (1+k)^l}{l!} \frac{\gamma_0 \exp(-\gamma_0 y) \exp(-k)}{h(y)} \frac{1}{((1+k)+\gamma_0)^{l+1}} {}_1F_1\left(l+1,1;\frac{\gamma_0^2 y}{(1+k)+\gamma_0}\right) dy. \tag{18}$$

- **Theorem 2.19.** The following formula expresses the average SNR change in the *practical* measurement based feedback channel equalization model assuming Nakagami fading as channel model:

$$\mathbb{E}\left[\frac{\mathrm{SNR}}{\gamma_s}\right] = \int_0^{\infty} \frac{1}{h(y)} \gamma_0 \frac{m^m}{(m+\gamma_0)^m} \exp(-\gamma_0 y) {}_1F_1\left(m,1;\frac{\gamma_0^2 y}{m+\gamma_0}\right) dy. \tag{19}$$

2.1.2 Phase error correction analysis of channel equalization

In the previous subsection, the amplitude gain and its fluctuation were investigated in the presence of channel estimation error supposing binary transmission. Nevertheless, this section presents the analysis of the channel estimation error as well, but focusing on the behaviour of the signal's phase. This effect was investigated assuming two basic modulation techniques, namely the BPSK and QPSK modulations that have exact, closed-form expressions for the channel capacity too.

In practice, reference signals are transmitted for appropriate communication to the receiver periodically, which is able to estimate the channel distortions. Therefore, the accuracy of channel equalization has a major effect on the quality of communication, i.e. how precisely the receiver is capable of recovering the transmitted data in different channel propagation circumstances. Numerous wireless systems apply this kind of channel equalization, which is called Pilot Symbol Assisted Modulation (PSAM). PSAM has been researched in the last two decades. However, due to new emerging and even more complex technologies, further investigations are necessary to improve their capabilities [5]-[8]. This is particularly true in term of 5G mobile networks that require even more sophisticated solutions.

Here, the statistical behaviour of the impact of channel estimation error on Symbol Error Ratio (SER) is analysed using pilot signals in a flat, non-frequency selective fading channel. As corollaries of theorems, the effective channel capacities for both BPSK and QPSK modulations are determined. The term of effective channel capacity means the ratio of pilot signals against the data signals. While pilot signals are required for proper channel estimation, they do not carry any useful information to the receiver. Therefore, this issue is rephrased as an optimization problem and further investigated in this section. At the end, the results are compared to the state-of-the-art LTE/LTE-A standard that uses QPSK modulated pilot signals for channel equalization.

THESIS I.5. [C1] *I described an analytical calculation method to determine the symbol error rate for BPSK and QPSK modulations taking into account the estimation error of the signal's phase assuming Rayleigh fading channel.*

The corresponding lemmas, theorems and corollaries from the dissertation are the following.

- **Lemma 2.1.** The phase rotating behaviour of the channel can be expressed by the following probability density function using polar coordinate system:

$$\begin{aligned} f_{\Phi}(\phi) = & \frac{1}{2\pi}\exp\left(-\gamma_s\right)\exp\left(\gamma_s\cos^2(\phi)\right)\sqrt{\frac{\pi}{2}} \\ & \left[\sqrt{\frac{2}{\pi}}\exp\left(-\gamma_s\cos^2(\phi)\right)+\sqrt{2\gamma_s}\cos(\phi)\right. \\ & \left.\left[1-\operatorname{erf}\left(-\sqrt{\gamma_s}\cos(\phi)\right)\right]\right], \end{aligned} \tag{20}$$

where $\gamma_s = E_s/N_0$ means the signal-to-noise ratio and $\operatorname{erf}(\cdot)$ is the Gauss error function.

- **Theorem 2.20.** The next formula expresses the symbol error rate assuming BPSK modulation in the pilot symbol assisted transmission system, when the presented signal phase equalization is used:

$$\begin{aligned} P_{s,BPSK}(\gamma_s,\gamma_0) =& \frac{1}{2\pi}\int\limits_{-\frac{\pi}{2}}^{\frac{\pi}{2}}\int\limits_{\frac{\pi}{2}+\phi}^{\frac{3\pi}{2}+\phi}\exp\left(-\gamma_0\frac{\sin^2\left(\frac{\pi}{2}+\phi\right)}{\sin^2\left(\frac{\pi}{2}+\phi-\theta\right)}\right)f_\Phi(\phi)d\theta d\phi + \\ &+\left(1-\frac{1}{2\pi}\int\limits_{\frac{\pi}{2}}^{\frac{3\pi}{2}}\int\limits_{-\frac{\pi}{2}+\phi}^{\frac{\pi}{2}+\phi}\exp\left(-\gamma_0\frac{\sin^2\left(-\frac{\pi}{2}+\phi\right)}{\sin^2\left(-\frac{\pi}{2}+\phi-\theta\right)}\right)f_\Phi(\phi)d\theta d\phi\right), \end{aligned} \tag{21}$$

where γ_s and γ_0 are the signal-to-noise ratios of the data and the pilot symbols and $f_\Phi(\phi)$ is the probability density function of the signals' phase rotation (Eq. 20).

- **Corollary 2.20.1.** The theoretical capacity of a BPSK modulated and pilot symbol assisted communication system is expressed as follows, when the presented signal phase equalization is used:

$$C_{BPSK} = 1 + p_{-1}\log p_{-1} + (1-p_{-1})\log(1-p_{-1}). \tag{22}$$

- **Theorem 2.21.** The symbol error rate of QPSK modulation is determined by the following formula assuming pilot symbol assisted communication system, when the presented signal phase equalization is used:

$$\begin{aligned} P_{s,QPSK}(\gamma_s,\gamma_0) =& \int\limits_{-\frac{\pi}{2}}^{\frac{\pi}{2}} p_s(\phi)f_\Phi(\phi)d\phi = \int\limits_{-\frac{\pi}{2}}^{\frac{\pi}{2}} p_{-\sqrt{2}}(\phi)f_\Phi(\phi)d\phi + \\ &+\int\limits_{-\frac{\pi}{2}}^{\frac{\pi}{2}} p_{j\sqrt{2}}(\phi)f_\Phi(\phi)d\phi + \int\limits_{-\frac{\pi}{2}}^{\frac{\pi}{2}} p_{-j\sqrt{2}}(\phi)f_\Phi(\phi)d\phi, \end{aligned} \tag{23}$$

where γ_s and γ_0 are the signal-to-noise ratios of the data and the pilot symbols, $f_\Phi(\phi)$ means the probability density function of the signals' phase rotation (Eq. 20), and

$p_{-\sqrt{2}}(\phi), p_{j\sqrt{2}}(\phi), p_{-j\sqrt{2}}(\phi)$ are represented by the following expressions:

$$
\begin{aligned}
p_{j\sqrt{2}}(\phi) &= \frac{1}{2\pi} \int_{\frac{\pi}{4}+\phi}^{\frac{3\pi}{4}+\phi} \exp\left(-\gamma_0 \frac{\sin^2\left(\frac{\pi}{4}+\phi\right)}{\sin^2\left(\frac{\pi}{4}+\phi-\theta\right)}\right) d\theta + \\
&\quad + \frac{1}{2\pi} \int_{\frac{3\pi}{4}+\phi}^{\pi} \left[\exp\left(-\gamma_0 \frac{\sin^2\left(\frac{\pi}{4}+\phi\right)}{\sin^2\left(\frac{\pi}{4}+\phi-\theta\right)}\right) - \exp\left(-\gamma_0 \frac{\sin^2\left(\frac{3\pi}{4}+\phi\right)}{\sin^2\left(\frac{3\pi}{4}+\phi-\theta\right)}\right)\right] d\theta, \\
p_{-\sqrt{2}}(\phi) &= \frac{1}{2\pi} \int_{\frac{3\pi}{4}+\phi}^{\pi} \exp\left(-\gamma_0 \frac{\sin^2\left(\frac{3\pi}{4}+\phi\right)}{\sin^2\left(\frac{3\pi}{4}+\phi-\theta\right)}\right) d\theta + \\
&\quad + \frac{1}{2\pi} \int_{\pi}^{\frac{5\pi}{4}+\phi} \exp\left(-\gamma_0 \frac{\sin^2\left(\frac{3\pi}{4}-\phi\right)}{sin\left(\frac{3\pi}{4}-\phi+\theta\right)^2}\right) d\theta, \\
p_{-j\sqrt{2}}(\phi) &= \frac{1}{2\pi} \int_{\frac{5\pi}{4}+\phi}^{\frac{7\pi}{4}+\phi} \exp\left(-\gamma_0 \frac{\sin^2\left(\frac{\pi}{4}-\phi\right)}{\sin^2\left(-\frac{\pi}{4}-\phi-\theta\right)}\right) d\theta + \\
&\quad + \frac{1}{2\pi} \int_{\pi}^{\frac{5\pi}{4}+\phi} \left[\exp\left(-\gamma_0 \frac{\sin^2\left(\frac{\pi}{4}-\phi\right)}{\sin^2\left(-\frac{\pi}{4}-\phi-\theta\right)}\right) - \exp\left(-\gamma_0 \frac{\sin^2\left(\frac{3\pi}{4}-\phi\right)}{\sin^2\left(\frac{3\pi}{4}-\phi+\theta\right)}\right)\right] d\theta.
\end{aligned}
\tag{24}
$$

- **Corollary 2.21.1.** The exact channel capacity of QPSK modulated transmission is the following:

$$C_{QPSK} = 2 + \sum_i p_i \log p_i, \tag{25}$$

where $p_i \in \left\{p_{-\sqrt{2}}, p_{j\sqrt{2}}, p_{-j\sqrt{2}}, 1-p_s\right\}$.

- **Lemma 2.2.** Assuming QPSK modulation based transmission only, the Long Term Evolution technology is comparable against the current system model. Furthermore, the exact number of necessary pilot signals can be determined taking into account the signal to noise ratio to maximize the throughput by using the following formula:

$$R \leq \frac{n-m}{n} C(m) = \frac{n-m}{n} \left(2 + \sum_i p_i \log p_i\right),$$

where n is the overall number of channel symbols, m is the number of pilot signals, $C(m)$ is the capacity of the channel (depending on m) and R indicates the effective channel capacity, i.e. the upper bound of available rate. Basically, the effective channel capacity

determines, how many information bits per symbol can be transmitted through the channel in average. The connection between the different SNR values can simply be given as $\gamma_0 = m \cdot \gamma_s$, i.e. the SNR of pilot signals is directly proportional to the SNR of the channel. Based on numerical calculations, the optimal m can be easily found.

2.2 Analysis of spread spectrum methods

The corresponding chapter from the dissertation presents all the investigations and results related to spread spectrum based communication. The chapter is separated into two main sections. First, the correlation peak detection of chirp spread spectrum based communication systems are analysed. By using the proposed sliding-and-tracking correlators in the receiver, faster and more reliable correlation peak detection can be achieved, than with traditional correlators. Then, a novel chirp spread spectrum technique is proposed that utilizes the results of the previous analysis. The new scheme combines the traditional CSS based communication with pulse position (PP) modulation. The system provides simultaneous data transmission to multiple mobile terminals in an efficient and sophisticated way.

This section introduces the second thesis group that contains four theses.

2.2.1 Correlation peak detection

For proper operation, the receiver has to synchronize with the incoming signal. This means timing synchronization, when the receiver needs to determine at which time instants the incoming signal has to be sampled, and carrier synchronization, when the receiver needs to adapt the frequency and phase of its local carrier oscillator with those of the received signal, too. The accuracy of synchronization has a major effect on the performance of the communication independently from the technology. However, if an unfriendly, but realistic wireless environment is assumed with low signal-to-noise ratio, fading, multipath propagation, in-system and out-system interference, then it is easy to understand, that the acquisition of synchronization parameters is difficult. Therefore synchronization should be considered in general as a challenging task.

Here, a simple synchronization scheme is proposed that applies two correlators, and its statistical behaviour related to correlation peak detection is analysed using binary chirp modulation via AWGN channel. The so-called sliding-and-tracking correlators enable to acquire overlapping noise components during the measurements, which means that these components are not statistically independent. The advantage of this property is taken into account during the calculation of correlation in order to reduce the error probability of correlation peak detection. The proposed correlator ensures higher accuracy for synchronization than using the legacy sliding correlator. The findings can be adapted for spread spectrum modulation based communication systems as well, where the autocorrelation function of the spectrum spreading code has only one well-determined peak, e.g. DS and FFH based technologies.

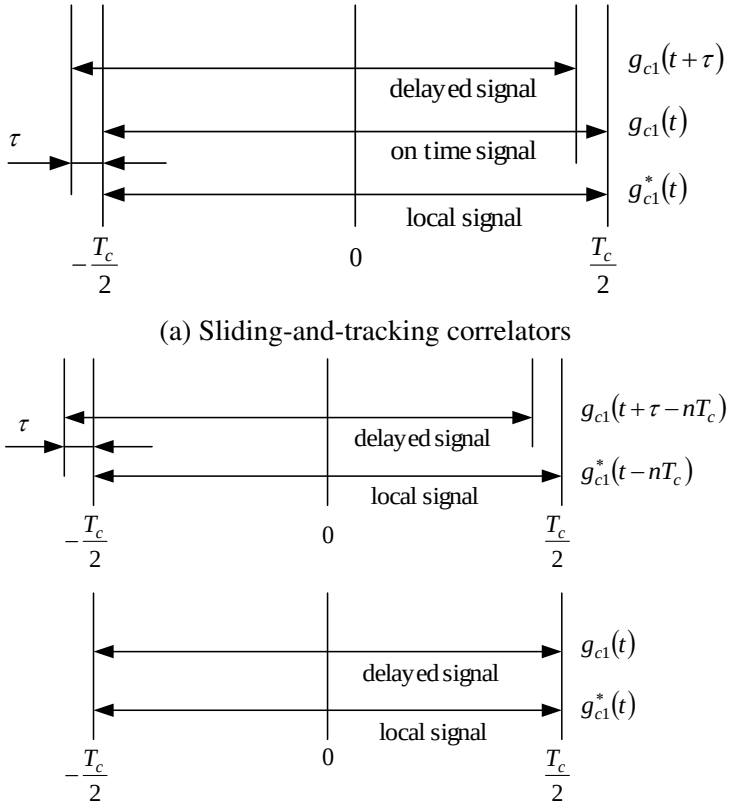

(a) Sliding-and-tracking correlators

(b) Sliding correlator

Figure 1: The integration domains of the different scenarios

Other possible application areas of the proposed method include the Ultra-wideband (UWB) and WLAN-based localization systems. There are several techniques available for localization [9], e.g. AoA (Angle of Arrival), ToA (Time of Arrival) and TDOA (Time Difference of Arrival), which require precise synchronization. Therefore the accuracy of positioning are closely related to the accuracy of synchronization.

THESIS II.1. [J2], [C2] *I defined a new method for detecting the correlation peak in such radio communication systems that have autocorrelation function with one well-determined peak.*

The idea of the proposed sliding-and-tracking correlators is depicted in Figure 1. As one can see, two, not independently operating correlators are applied that have overlapping time windows. So, the accumulated noise will appear in both correlators in the overlapped time. This feature enable to handle the additive white Gaussian noises as dependent random variables.

THESIS II.2. [J2], [C2] *I introduced an analytical method for calculating the bit error rate of the correlation peak detecting mechanism provided in Thesis II.1.*

The goal of the receiver is the detection of the correlation function maximum at $\tau = 0$ position. This means noncoherent measuring of the correlation function's values that belong to 0 and τ delays, and then deciding on the greater of them. It is assumed that the transmitter sends a training sequence, e.g. $g_{c1}(t)$ to the receiver till the synchronization is not finished. Note that the synchronization is possible without training sequence. The statistical properties of the depicted scheme are investigated in two scenarios.

In the first scenario, it is supposed that 0 and τ delays of $z_1(0)$ and $z_1(\tau)$ values are generated in overlapping time windows, i.e. two correlators are used, a sliding and a tracking correlator at the same time. This is illustrated by Figure 1a. The integration domain of the correlators are normalized to $[-T_c/2, T_c/2)$, but it is assumed that the incoming signal of one correlator is received in appropriate synchronous position and the other correlator gets it with τ delay. In this system, the two correlation calculations are evaluated in overlapping time windows, where the AWGN noises are not independent from each other, i.e. the results of the correlation are dependent random variables.

In the second scenario, it is supposed that the measurements of 0 and τ delays are performed in non-overlapping time windows, i.e. sliding correlators are applied for the detecting the maximum position. Figure 1b shows this second case. The integration domain of the correlators are also normalized to $[-T_c/2, T_c/2)$. Furthermore, it is assumed that the incoming signal of one correlator is received in appropriate synchronous position, but the other one receives it with $\tau - nT_c$ delay, i.e. the two correlation calculations are evaluated in non-overlapping time windows, thus the results of the correlation are independent RVs.

The corresponding theorems from the dissertation are listed below.

- **Theorem 3.1.** The wrong decision probability is determined by the following formula in case of noncoherent *sliding-and-tracking* correlators:

$$\begin{aligned} \mathbb{P}\{X_1 < X_2\} &= \int_0^\infty \int_x^\infty f_{XX_2}(x, x_2)\, dx_2 dx = \\ &= \sum_{k=0}^{\infty} \sum_{l=0}^{\infty} \frac{|\rho|^k}{2^{l+1}} \left(1-\rho^2\right)^{\frac{1}{2}(l+1)} \gamma^l \exp(-\gamma) \frac{(k+l)!}{(l!)^2} P_l^{-k}\left(\frac{1}{\sqrt{1-\rho^2}}\right), \end{aligned} \tag{26}$$

  where γ is the SNR and ρ is the correlation parameter given by the following expression:

$$\rho = \left(1 - \frac{|\tau|}{T_c}\right) \frac{\sin\left(\pi \Delta f\, |\tau| \left(1 - \frac{|\tau|}{T_c}\right)\right)}{\pi \Delta f\, |\tau| \left(1 - \frac{|\tau|}{T_c}\right)}. \tag{27}$$

- **Theorem 3.2.** The probability of the wrong decision is determined by the following

expression using noncoherent *sliding* correlators:

$$\mathbb{P}\{X_1 < X_2\} = \int_0^\infty \int_x^\infty f_{XX_2}(x, x_2)\, dx_2 dx = \sum_{k=0}^{\infty} \exp\left(-\left(1+\rho^2\right)\gamma\right) \int_0^\infty \exp(-2x) \left(|\rho| \sqrt{\frac{\gamma}{x}}\right)^k I_0\left(2\sqrt{\gamma x}\right) I_k\left(2|\rho|\sqrt{\gamma x}\right) dx. \tag{28}$$

- **Theorem 3.3.** The wrong decision probability is determined by the following expression in case of coherent *sliding-and-tracking* correlators:

$$\mathbb{P}\{X_1 < X_2\} = \frac{1}{2}\mathrm{erfc}\left(\sqrt{\frac{\gamma}{2}(1-\rho)}\right). \tag{29}$$

- **Theorem 3.4.** The wrong decision probability is determined by the following formula in case of coherent *sliding* correlators:

$$\mathbb{P}\{X_1 < X_2\} = \frac{1}{2}\mathrm{erfc}\left(\sqrt{\frac{\gamma}{2}(1-\rho)^2}\right). \tag{30}$$

2.2.2 Multi-user chirp spread spectrum technique

The last decade of telecommunication was about the increasing demand of higher data throughput and lower latency. However, as the focus changes from humans to machines, different requirements arise meaning that not every application needs high throughput. Reliable and robust communication is much important for these certain applications. Such possible applications are on the field of Industry 4.0 or smart agriculture, where reliable, but simple controlling of remote devices, automated vehicles or drones does not necessarily need high speed data connection. From a more general aspect the Internet of Thing is also a possible usage area of such Low-Power Wide-Area Networks, where similar requirements have to be fulfilled. For these applications, the wireless communication system can be based on spread spectrum techniques, which are quite simple and matured, but do not provide so high data transfer rates, than the nowadays popular Orthogonal Frequency-Division Multiplexing (OFDM) variants.

The spread spectrum techniques are known long ago and used by many different standards in vast of communication devices. Direct-Sequence Spread Spectrum and Frequency-Hopping Spread Spectrum techniques are used in numerous widely spread standards. The usage of DSSS includes the IEEE 802.11b standards, as the original Wi-Fi system; the IEEE 802.15.4 standard, which is the physical layer for ZigBee; the Code Division Multiple Access (CDMA) channel access method; and also it is integral part of different Global Navigation Satellite Systems (GNSS), like GPS, GLONASS and Galileo. FHSS can be familiar from Bluetooth, where its variant is used known as Adaptive Frequency-hopping spread spectrum.

Maybe, the Chirp Spread Spectrum based systems are not so well-known for the average user as other spread spectrum methods, but its benefits include high robustness against channel

noise, interference and jamming. Furthermore, the resistance capability against the Doppler effect makes the CSS a very good candidate in such mobile communication environments, where support for terminals moving with high speeds and at long ranges is necessary. These reasons were led to standardize CSS as one of the supported physical layer of IEEE 802.15.4a for use in Low-Rate Wireless Personal Area Networks [10][11]. Its variants are also standardized in the last year for Long Range Wide Area Network, which is an emerging technology for LPWAN communication [12][13].

The corresponding section of the dissertation presents a new mobile communication system based on Chirp Spread Spectrum transmission. The downlink modulation scheme is extended with Pulse Position Modulation (PPM) to carry data for multiple mobile terminals simultaneously. The described novel mechanism ensures reliable and robust communication between the parties, especially for terminals moving with high speeds or at long range. Furthermore, the proposed system takes care of the uplink communication as well, where Closed-Loop Power Control is applied to handle the near-far problem and improve the performance of the system. Analytical investigations for downlink communication are described focusing on the instantaneous symbol error rate and average SER in Rayleigh fading channel. The results show that the proposed Multi-User Pulse Position based Chirp Spread Spectrum technique (shortly MU-PP-CSS) allows higher data rates that are used for the multi-user feature.

THESIS II.3. [C3] *I described a novel mobile communication system that can use two slightly different multi-user technique for downlink that combine pulse position modulation with chirp spread spectrum based mobile transmission scheme. Furthermore, they apply the CLPC method according to Thesis I.3. in uplink.*

The related definitions and theorems from the dissertation are the following.

- **Definition 3.1.** I developed a novel radio communication system that provides low-power wide area transmission for mobile terminals. It uses the MU-PP-CSS technique for downlink and PP-CSS for uplink communication, as well as it utilizes the measurement based closed loop power control mechanism to mitigate near-far problem.

  Assume a communication system that provides wireless connectivity between a base station (BS) and mobile terminals (MT). The available bandwidth of the system is fully utilized by Chirp Spread Spectrum transmission, where the signals are modulated by chirp pulses, i. e. frequency varying sinusoidal pulses. To simplify the RF circuit design, time-division duplexity is applied in the scheme to separate the downlink and uplink communication. The downlink is based on the MU-PP-CSS technique, while the system applies PP-CSS on the uplink with measurement based CLPC method.

- **Definition 3.2.** To extend the downlink chirp spread spectrum communication with pulse position modulation, framing is necessary in order to the terminals be able to distinguish the transmitted bits from the BS. Here, it is supposed that the elementary down-chirp

signal is applied to indicate the starting of the frame, however, it is also possible to use the up-chirp signal for this purpose.

Let $g_{c0}(t)$ the elementary signal for frame synchronization and $g_{c1}(t), g_{c2}(t), ..., g_{ci}(t), ..., g_{c2^M}(t)$ the elementary signals for data symbols in the non-binary pulse position based chirp modulation system. The next expression describes the low-pass equivalent *complex-valued* representations of these signals related to MU-PP-CSS variant A:

$$\begin{aligned} g_{c0}(t) =& A \exp\left(-j2\pi \frac{\Delta f}{2T_c}(t-\tau_0)^2\right), \quad (t-\tau_0) \in \left[-\frac{T_c}{2}, \frac{T_c}{2}\right) \\ g_{ci}(t) =& A \exp\left(j2\pi \frac{\Delta f}{2T_c}(t-\tau_i)^2\right), \qquad (t-\tau_i) \in \left[-\frac{T_c}{2}, \frac{T_c}{2}\right) \end{aligned} \tag{31}$$

where A is the amplitude of the elementary signals, Δf is the chirp modulated signal's frequency spreading domain, T_c is the frequency varying sinusoid signal's symbol time, τ_i is the delay related to the time position of each symbol, $i = 1, ..., 2^M$ is the symbol number and $2^M + 1$ is the overall number of the available symbols in the system. M is referred as the data rate parameter.

- **Definition 3.3.** Instead of mapping the time-shifted signals to binary words, which then are bitwise or partially assigned to the mobile terminals, the idea is to map the time-shifts directly to MTs. One τ delay is required to be associated to a terminal, the up- and down-chirps related to the given delay as pairs carry the binary information for the MT. In other words, in this case the base station is able to send M number of different time-shifted up- and down-chirp signals, however, only one mobile terminal will receive one bit information depending on the τ-shift. The exact value of the binary information is decided based on the direction of the given, transmitted signal. Framing is not necessary in this variant. The low-pass equivalent *complex-valued* representations of the signals of MU-PP-CSS variant B are given as

$$\begin{aligned} g_{ci_1}(t) =& A \exp\left(-j2\pi \frac{\Delta f}{2T_c}(t-\tau_i)^2\right), \quad (t-\tau_0) \in \left[-\frac{T_c}{2}, \frac{T_c}{2}\right) \\ g_{ci_2}(t) =& A \exp\left(j2\pi \frac{\Delta f}{2T_c}(t-\tau_i)^2\right), \qquad (t-\tau_i) \in \left[-\frac{T_c}{2}, \frac{T_c}{2}\right) \end{aligned} \tag{32}$$

where $i = 1, ..., M$ is the symbol number and $2M$ is the overall number of the available symbols in variant B. Other notations are the same as in Eq. 31.

- **Definition 3.4.** In the proposed communication system, the same signals are used for the uplink transmission. However, the common channel is shared in time between the mobile terminals in this case. Since the symbol synchronization is defined by the base station, each MT transmits in its own, dedicated time slot using pulse position based chirp spread

spectrum modulation. The $i-th$ mobile terminal can send its binary information using the assigned elementary signals. According to MU-PP-CSS variant A, these signals can be the up-chirps starting with different time delays (Eq. 31) or they can be both up- and down-chirps with identical time-shift in case of variant B (Eq. 32). Hence, the overall throughput of MTs is M. Furthermore, measurement based feedback CLPC mechanism is applied in the uplink to overcome the near-far problem.

- **Theorem 3.5.** The PP-CSS transmission method uses quasi-orthogonal chirps as elementary signals that can be considered orthogonal practically.

- **Theorem 3.6.** The quasi-orthogonal property of the chirp signals in PP-CSS transmission technique is still valid, if additive white Gaussian noise is assumed in the communication channel.

THESIS II.4. [C3] *I provided analytical calculation method to determine the bit error rate of the multi-user schema described in Thesis II.3. assuming Rayleigh fading channel.*

The corresponding formulas from the dissertation are listed below.

- **Equation 3.22** Due to the non-coherent receiver structure of MU-PP-CSS, the following general expression for non-coherent reception in AWGN channel can be applied from [14]:

$$P_{SER_{DL}} = \sum_{m=1}^{2M-1} (-1)^{m+1} \binom{2M-1}{m} \frac{1}{m+1} \exp\left(-\frac{E_s}{N_0} \frac{m}{m+1} \right),$$

  where $P_{SER_{DL}}$ is the symbol error rate for downlink.

- **Equation 3.23** Beside the instantaneous SER, the average SER can be determined for slow, frequency non-selective Rayleigh fading channel by the following formula based on [14]:

$$\overline{P}_{SER_{DL}} = \sum_{m=1}^{2M-1} (-1)^{m+1} \binom{2M-1}{m} \frac{1}{m+1} \frac{1}{1+\frac{m}{1+m}\frac{\overline{E}_s}{N_0}},$$

  where $\overline{E}_s$ is the average symbol energy of the signal and $\overline{P}_{SER_{DL}}$ is the average SER for downlink.

- **Equation 3.24** The instantaneous symbol-error rate is the following:

$$P_{SER_{UL}} = \frac{1}{2} \exp\left(-\frac{E_s}{2N_0} \right),$$

  where $P_{SER_{UL}}$ is the symbol error rate for the uplink communication.

- **Equation 3.25** Similarly, the average SER in slow, frequency non-selective Rayleigh fading channel is expressed as

$$\overline{P}_{SER_{UL}} = \frac{1}{2+\frac{\overline{E}_s}{N_0}},$$

where $\overline{P}_{SER_{UL}}$ is the average SER of uplink.

- **Equation 3.26** For extensive investigations, the influence of the quasi-orthogonality on the demodulator has to be analysed as well. In other words the operation of the receiver has to be investigated, when the correlation of the two elementary signals $g_{c_1}(t)$ and $g_{c_2}(t)$ is ρ. The solution of this problem is known from [14] for the channel without fading:

$$P_b = \left[\sum_{k=0}^{\infty} \left(\frac{1-\sqrt{1-\rho^2}}{1+\sqrt{1-\rho^2}} \right)^{\frac{k}{2}} \times I_k \left(|\rho| \times \frac{E_b}{2N_0} \right) - \frac{1}{2} I_0 \left(|\rho| \times \frac{E_b}{2N_0} \right) \right] \times \exp\left(-\frac{E_b}{2N_0} \right),$$

where P_b is the bit error rate and $I_k(\cdot)$ is the k-th order modified Bessel function.

- **Equation 3.27** The bit error rate of the proposed measurement based feedback power control mechanism assuming Rayleigh fading channel is given as follow

$$P_{b_{CLPC}}(\gamma_s) = \int_0^{\infty} \frac{1}{h(y)} \frac{\gamma_0}{1+\gamma_0} \exp\left(-\frac{\gamma_0}{1+\gamma_0} y \right) dy, \tag{33}$$

where $P_{b_{CLPC}}(\gamma_s)$ is the average BER, γ_s is the SNR of the channel, γ_0 is the SNR of the pilot signal, y describes the stochastic process of the fading parameter estimation:

$$Y = \left| z + \frac{\overline{n}}{\sqrt{E_0}} \right|^2,$$

and the $h(x)$ function introduces the threshold value related to the maximum transmission power of the mobile terminals:

$$h(x) = \begin{cases} c & \text{if } |x| \leq c \\ x & \text{if } |x| > c \end{cases}$$

Basically, the equation of $P_{b_{CLPC}}(\gamma_s)$ represents the behaviour of the uplink communication taking into account the limitations of the mobile terminals regarding their transmission power and the estimation error due to the imperfect reception of the pilot (i. e. the frame synchronizing down-chirp) signal.

2.3 Analysis of handover process in two-tier LTE/LTE-A

Data and voice traffic increases continuously day by day, more and more percentage of that is handled by mobile equipment. The forecasts show significant growth of mobile subscribers thanks to connecting new markets and spread of smart applications using Machine-to-Machine (M2M) communication. To tackle this issue, new trends are emerging in next generation mobile networks. More precisely, bringing the base stations closer to users, providing better coverage and better QoS are quite new aspects in cellular networks. The so-called small cells or femtocells are low transmit power access points with relatively small coverage ($\sim$ 30 meters) operating in licensed spectrum. A realization of the small cell concept is included in the 3GPP Long Term Evolution - Advanced (LTE-A) standard, namely in form of the Home evolved-NodeBs (HeNB) [15]. The HeNBs have the opportunity to provide sufficient signal strength to proximity users and better coverage inside the buildings along with cheap and easy installation. The femtocell user generated traffic is forwarded to the mobile operator via wired techniques (xDSL, cable etc.). The small cells have three different access modes to be in line with market demands. In open access mode, every potential user equipment (UE) can connect to femtocell, while in closed access mode just a group of users is allowed to join, i.e. the UE's ID have to be on the femtocell's so-called closed subscriber group (CSG) list. The UE also stores the CSG IDs of the allowed small cells. Finally, the hybrid access mode is the combination of the previous two sharing the radio resource between the CSG and non-CSG users. In this case the CSG users have the advantage in the service. The main drawback of using the small cells is the user installation, which means uncontrolled interference source and independent operation from the service providers. From another aspect, the operator can also install small cells to either indoor (e.g. offices) and outdoor (e.g. utility or lamp poles) locations. The benefit of the latter solution beyond from the aforementioned is the manageability by the service provider. The implementation of the small cell is supported by the LTE-A introducing a new entity (HeNB Gateway) in E-UTRAN (Evolved Universal Terrestrial Radio Access Network).

In two-tier macrocell-small cell LTE-A, one key feature is the mobility management, i.e. the seamless switch from one base station to another, which is in the focus of the related chapter. Many papers were published in the recent years proposing more and more sophisticated solutions of the handover (HO) decision procedure [J4]. Numerous from these use different network provided information during the decision that are typically not included in the standard, e.g. the velocity of user equipment, RSSI (Received Signal Strength Indicator), load information of cells, access type of HeNBs etc.

In the corresponding chapter of the dissertation a new handover decision algorithm for the two-tier macrocell-small cell LTE-A network is described. The algorithm uses positioning service and takes into account different network provided information, namely the reported RSSI values, the speed of the users and the actual load of the base stations. In addition, a sliding averaging window on the RSSI values is applied to enable the filtering of the instantaneous fluctuation of the radio channel and avoid unnecessary cell changing.

The two-tier architecture means that the network has two different layers, which are the fol-

lowings: the layer of the eNodeBs (eNB) as the first, macrocell tier and the layer of the HeNBs as the second, femto or small cell tier. The introduction of small cells affects the operation and the architecture of LTE/LTE-A. In the earlier releases of the standard [15], the E-UTRAN has been completed with an additional entity named as HeNB Gateway (HeNB GW). The HeNB GW is optional, but if present, acts as an eNB to the Mobility Management Entity (MME) and appears as an MME to a HeNB. It serves as a concentrator for the control plane, thus it has the ability to support a large number of HeNBs in a scalable manner. The X2 interface provides the direct connection between the cells independently whether they are eNBs or HeNBs. The X2-based HO between small cells is not allowed only if access control at the MME is necessary, i.e. if the UE handovers from a closed/hybrid access HeNB to a closed access HeNB with different CSG ID.

THESIS III.1. [J3], [C4], [C5] *I defined a new hybrid handover decision algorithm for two-tier LTE/LTE-A network, and investigated its efficiency by simulations.*

The corresponding definition from the dissertation is the following.

- **Definition 4.1.** I developed a novel handover decision algorithm for two-tier LTE/LTE-A system that takes into consideration the velocity of the UE, the access mode of the small cells and received signal strength indicator extended by hysteresis margin. It is able to increase the overall system throughput and reduce the user latency compared to the legacy decision procedure.

It is assumed that the network can determine the geographic position and velocity of user equipment based on measuring radio signals. The standard gives the opportunity to do that providing different techniques [16] and protocol [17].

The pseudo code of the proposed algorithm is described in Algorithm 1. The basic idea of the method is making a list of the possible target cells based on the reported RSSI values using the sliding averaging window and the Handover Hysteresis Margin (HHM) (see line 3-9). Then, this list is sorted by taking into account the access modes (in order of closed, hybrid, open access modes), the actual load (the lowest the best) and the RSSI of the target (H)eNBs (the highest the best) (line 13). Finally, the first base station from the list is selected as the target cell (line 15-16). If the HO is prevented by radio failure or the MME (e.g. the UE does not have access to the given HeNB), the UE is directed to the next cell on the list (line 17-18). The speed values are used to decide whether the UE is allowed to handover to the target cell on the list or it has to switch to the macrocell with the highest RSSI value (line 10-11). This function ensures that a faster user cannot get stuck at a cell. Note that an overall eNB coverage is assumed here.

Higher QoS is expected, i.e. higher system throughput and lower user latency due to the load balancing effect caused by the higher priority of the actual load over the RSSI during the list sorting. One can assume a scenario, where two open access HeNBs are close together. In case of the legacy algorithm, the closer cell will be chosen because of the Strongest Cell decision policy, hence, the balancing is not guaranteed. However, with the proposed algorithm the UE

Algorithm 1 The hybrid handover decision algorithm

Require: *RSSI* values with (H)eNB IDs from the measurement report of the UE

Initialize the HHM, the speed threshold v_{th} and the possible target (H)eNB list L for the UE
Calculate/collect the speed of the UE v, the current serving (H)eNB RSSI $RSSI_{current}$ and the eNB ID with the highest RSSI *max eNB*
for all i in *RSSI* **do**
    Update the sliding averaging window of the i^{th} (H)eNB with $RSSI_i$
    Calculate the new average avg_i
    if $avg_i \geq RSSI_{current} + HHM$ **then**
        Add i to the end of L
    end if
end for
if $v \geq v_{th}$ **then**
    Initialize HO to *max eNB*
else
    Sort the list by access mode, actual load and RSSI
    repeat
        Get the first (H)eNB $l_{1^{st}}$ from L
        Initialize HO to $l_{1^{st}}$ from L
        Erase $l_{1^{st}}$ from L
    until HO is not successful or the list is not empty
end if

will switch to the small cell with less load, e.g. with less served mobile and will get more radio resource, therefore the QoS of the UE will be higher.

Note that a trade-off should be found between selecting the strongest cell, thus communicating on less resource with better transport format (i.e. with better modulation and coding) and selecting the cell with less load, i.e. having more resource but worse radio channel quality, hence worse transport format. Taking into account this consideration, the proposed algorithm will work better in those scenarios, where the small cells are placed randomly and the aforementioned case (two HeNBs are close together) can occur. Assuming the user installation of HeNBs, their locations can modelled as a random process.

3 Application of results

The dissertation describes all my research and scientific contribution from the recent years. I structured the dissertation into three main chapters reflecting my three main research areas. First, the channel equalization related investigations are introduced. I presented a novel method for channel equalization, namely the measurement based feedback channel equalization that is considered as a closed loop power control mechanism. It compensates the amplitude fluctuation of the transmitted signal that is caused by the fading in the radio channel. The method assumes that the equalization is executed by the transmitter based on the measured and feedback information from the receiver. I introduced new formulas regarding to the bit error rate of the system taking into account different fading models, such as Rayleigh, Rician and Nakagami for both coherent and noncoherent receptions. The expressions might look difficult, but they are able to simplify the BER calculations, as well as the formulas are derived to closed form in some cases. It also has to be highlighted that in each case the maximum output power of the transmitter is considered as a limitation factor, since infinite compensation of the channel distortions is not possible in practice. Later, it is shown that this model and the related expressions are applicable for practical communication systems, i.e. the Pulse Position based Chirp Spread Spectrum scheme is capable of utilizing the presented CLPC mechanism.

In addition, investigations were carried out related to pilot signal assisted systems, in which the estimation error of the reference signals influences the symbol error rate of the whole system. Formulas are determined assuming BPSK and QPSK modulations that suffer from phase measurement error due to fading. Furthermore, the analysis is turned into a channel capacity optimization problem, where the trade-off has to be found between the number of pilot and data signals. Considering LTE/LTE-A network, the optimal number of reference symbols are determined taking into account the signal-to-noise ratio of the communication channel. The results could be used during the standardization of the LTE/LTE-A, however, the 3GPP 5G New Radio can also profit from them, since it supports the flexible allocation of reference signals.

Then, the third chapter of the dissertation describes the spread spectrum techniques related investigations. First, a new synchronization method is presented that is based on the sliding-and-tracking correlators. The basic idea is that if two correlators are used in overlapping time window, then significant part of the noise will appear twice in the output of the correlators, and therefore it can be handled as non-independent random variables during the correlation calculations. The analysis covers both coherent and noncoherent receptions, and provides expressions related to the wrong decision probabilities.

The second section of the third chapter is about a novel communication scheme that uses pulse position modulation over chirp signals to enable simultaneous transmission for multiple mobile terminals. Two, slightly different variants are presented as the downlink communication, while the interesting part of the uplink is the earlier proposed CLPC mechanism that effectively manages the near-far problem. Formulas are derived regarding to the feasibility (quasi-orthogonality feature of the scheme), as well as the downlink and uplink performance.

Finally, the forth chapter of the dissertation introduces a novel handover decision algorithm for two-tier LTE/LTE-A system that takes into account the velocity of the user equipment, the load and the RSSI of the candidate cells, as well as their access mode. Therefore, the algorithm results a more balanced distribution of UEs between the base stations, while it provides higher system throughput and lower latency especially in such scenarios, where the small cells are deployed randomly.

3.1 Outlook

There are several ways to improve or extend the presented investigations. Regarding to the measurement based feedback channel equalization, expressions can be derived for more fading models like Weibull fading, as well as additional systems could be found that can apply the proposed model. Considering the analysis of the phase error, expressions can be determined for 8-PSK modulation. Furthermore, it should be investigated if the generalization of formulas is possible, thus one formula could cover all PSK based modulations. A further extension of the work is about the detailed investigation of 5G New Radio system, in which the reference signals are differentiated based on their purpose, and they are usable in a more scalable, flexible way. However, the standard itself does not determine any exact relationship between the number and type of signals and the channel conditions.

The new synchronization technique provided by the sliding-and-tracking correlators should be built and investigated in practice. So, the analytical results can be compared to real measurements, and the accuracy of the expression can be analysed. Similarly, the pulse position based chirp spread spectrum could be implemented using software radio platforms, and then the performance related properties can be measured and investigated. As mentioned, CSS based communication is quite robust and reliable for long distances as well. Due to the proposed novel multi-user schema, a bit less transmission range is foreseen that could be properly determined with practical measurements. Since the chirp signal is insensitive to Doppler-effect, the mobile terminals can move with high speeds. The equalization of the uplink chirp signals are taken care by the proposed CLPC mechanism. As exploitation, patenting the PP-CSS should be considered.

Finally, a lot of knowledge were acquired regarding to the handover procedure in 4G LTE/LTE-A network. By introducing the concept of small cells in the 3GPP standards, a new situation was created in the network, which was investigated by many researchers including me. However, the home eNodeBs are not really spread, probably due to its drawbacks, and of course the mobile network operators are not really like to lose their influence over their network and especially over their licensed spectra. Nevertheless, the 5G New Radio has similar handover procedure, but the whole network concept is matured. This means that multi-tier and multi-RAT operations are natural, and including new types of end users (machines, vehicles) enables further investigations based on this knowledge.

4 List of Publications

Published peer-reviewed journals

[J1] Ádám Knapp, László Pap, *"General Performance Analysis of Binary Fading Channels with Measurement Based Channel Equalization"*, INFOCOMMUNICATIONS JOURNAL VI:(1) pp. 1–9. 2014, (indexed in **Scopus**)

[J2] Ádám Knapp, László Pap, *"Statistical analysis of a new correlation peak detection method for unimodal autocorrelation"*, COMPUTER COMMUNICATION & COLLABORATION 3:(1) pp. 63–81. 2015.

[J3] Ádám Knapp, László Pap, *"A novel mobile communication system using Pulse Position based Chirp Spread Spectrum modulation"*, Journal of Communications Software and Systems, Vol.14, No.3 (2018), pp. 228–238, Sept. 2018. (indexed in **Scopus**)

[J4] Győző Gódor, Zoltán Jakó, Ádám Knapp, Sándor Imre, *"A Survey of Handover Management in LTE-based Multi-tier Femtocell Networks: Requirements, Challenges and Solutions"*, Elsevier Computer Networks, Vol. 76, No. C, pp. 17–41, 2015, (indexed in **Scopus**, **WoS**)

Conference articles

[C1] Ádám Knapp, László Pap, *"Statistical based optimization of number of pilot signals in LTE/LTE-A for higher capacity"*, EUROCON 2015 – International Conference on Computer as a Tool, Salamanca, Spain, 2015, pp. 1–5, ISBN: 978-1-4799-8569-2, DOI: 10.1109/EUROCON.2015.7313768

[C2] Ádám Knapp, Pap László, *"A new synchronization method for direct sequence spectrum spread based systems"*, Proceedings of the 5th International Conference on Recent Achievements in Mechatronics, Automation, Computer Sciences and Robotics 2015 (MACRo 2015). Târgu Mures, Romania, 2015, pp. 37–48.

[C3] Ádám Knapp, László Pap, *"Performance Analysis of Pulse Position based Chirp Spread Spectrum technique for Multiple Access"*, 2017 25th International Conference on Software, Telecommunications and Computer Networks (SoftCOM), Split, Croatia, 2017, pp. 1–5, DOI: 10.23919/SOFTCOM.2017.8115574 (**Best paper award**)

[C4] Ádám Knapp, Zoltán Jakó, *"Hálózati térkép alapú hívásátadási eljárás kétrétegű LTE-ben"*, Tavaszi Szél 2014 / Spring Wind 2014 VI. pp. 183–191., Debrecen, Hungary, 2014. ISBN: 978-615-80044-4-2

[C5] Ádám Knapp, Győző Gódor, *"The effect of a new hybrid decision handover algorithm on QoS in two - tier LTE - A network"*, 22nd Conference on Software, Telecommunications and Computer Networks (SoftCOM 2014), Split, Croatia, 2014, pp. 331–335. DOI: 10.1109/SOFTCOM.2014.7039126

Other publications (not related to theorems)

[C6] Zoltán Jakó and Ádám Knapp, *"Business Scenarios and Data Flow in NeMo Hyper-Network"*, 2018 International Conference on Smart Systems and Technologies (SST), Osijek, 2018, pp. 139-144. DOI: 10.1109/SST.2018.8564701

[C7] Fatemeh Bardestani, Zoltán Jakó, Ádám Knapp, Sándor Imre, Péter Fazekas, *"Improving Wireless Network Throughput with Constant Dimension Subspace Codes"*, 9th IEEE, IET Int. Symposium on Communication Systems, Networks and Digital Signal Processing (CSNDSP 2014), Manchester, United Kingdom, 2014, pp. 508–512.
DOI: 10.1109/CSNDSP.2014.6923882

[C8] Ádám Knapp, Sándor Imre, Zoltán Jakó, Gábor Jeney, *"Application of LTE Small Cells in Urban Environments for Higher Capacity"*, 19th IEEE International Conference on Networks (ICON 2013), Singapore, 2013.12.11-2013.12.13, pp. 1–6.
DOI: 10.1109/ICON.2013.6781965

[C9] Ádám Knapp, Sándor Imre, Zoltán Jakó, Gábor Jeney, *"Average System Capacity in a Two-tier LTE Environment with Random Waypoint Mobile Users"*, 18th IEEE International Conference on Networks (ICON 2012), Singapore, 2012, pp. 36–40.
DOI: 10.1109/ICON.2012.6506530

[C10] Ádám Knapp, *"Simulation Analysis of the Long Term Evolution"*, Proceedings of the 15th International Student Conference on Electrical Engineering. Prague, Czech Republic, 2011, Paper C09.

[BC1] Zoltán Jakó, Ádám Knapp, Lajos Nagy, András Kovács, *Cooperative Intelligent Transport Systems: Towards High-Level Automated Driving – Chapter 8: Vehicular communication – a technical review*, 1st edition, IET Digital Library, 2019. (Unpublished, expected publication date: Sept. 2019)

4.1 Publication Summary

- Journal paper: 4; 17.5 points
  - 4 in English, peer-reviewed journal (1 in WoS, 2 in Scopus databases)
- Conferences: 10; 14.6 points
- Book chapter: 1; 3 points
- **Total points**: **35.1 points**
- Publications in SCI (WoS): 1; [J4]

References

[1] G. L. Stuber, *Principles of Mobile Communication*, 2nd ed. Norwell, MA: Kluwer, 2001.

[2] Andrews, J.G.; Buzzi, S.; Wan Choi; Hanly, S.V.; Lozano, A.; Soong, A.C.K.; Zhang, J.C., "What Will 5G Be?", *IEEE Journal on Selected Areas in Communications*, Vol. 32, No. 6, pp. 1065-1082, June 2014.

[3] J. Rodriguez, *Fundamentals of 5G Mobile Networks*, 1st edition, John Wiley & Sons, 2015.

[4] A. Osseiran *et al.*, *5G Mobile and Wireless Communications Technology*, Cambridge University Press, 2016.

[5] Simko, M.; Pendl, S.; Schwarz, S.; Qi Wang; Ikuno, J.C.; Rupp, M., "Optimal Pilot Symbol Power Allocation in LTE," *2011 IEEE Vehicular Technology Conference (VTC Fall)*, pp. 1-5, Sept. 2011.

[6] Omri, A.; Hamila, R.; Hasna, M.; Bouallegue, R., "Dynamic optimization of LTE pilot scattering based on channel estimation," *2012 International Conference on Computer & Information Science (ICCIS)*, pp. 558-562, June 2012.

[7] Yiji Lei; Heng Liu, "Optimal LTE-A pilot patterns and numbers of MIMO transmission streams under high mobility scenarios," *2014 International Workshop on High Mobility Wireless Communications*, pp. 43-47, Nov. 2014.

[8] Bouchibane, F.Z.; Ghanem, K.; Bensebti, M., "Performance analysis of pilot pattern design for channel estimation in LTE downlink," *2014 IEEE Antennas and Propagation Society International Symposium (APSURSI)*, pp. 408-409, July 2014.

[9] H. Liu, H. Darabi, P. Banerjee and J. Liu, "Survey of Wireless Indoor Positioning Techniques and Systems," *IEEE Transactions on Systems, Man, and Cybernetics, Part C (Applications and Reviews)*, vol. 37, no. 6, pp. 1067-1080, Nov. 2007.

[10] E. Karapistoli *et al.*, "An overview of the IEEE 802.15.4a standard," *IEEE Communications Magazine*, vol. 48, no. 1, pp. 47-53, January 2010. DOI: 10.1109/MCOM.2010.5394030

[11] IEEE 802.15.4-2011 Standard, http://www.decawave.com/technology/ieee802154a-standard

[12] LoRa Alliance, *LoraWAN Specification*, V1.0.2, July 2016.

[13] Mobile Experts, *White Paper for LoRa Alliance*, April 2016.

[14] John Proakis and Masoud Salehi, *Digital Communications*, 5th edition, McGraw-Hill, November 2007, ISBN: 0072957166.

[15] 3GPP TS 36.300 V12.1.0 (2014-03) E-UTRA, E-UTRAN, Overall Description; Stage 2 (Release 12)

[16] 3GPP TS 36.305 V12.3.0 (2013-12), Stage 2 functional specification of User Equipment (UE) positioning in E-UTRAN (Release 12)

[17] 3GPP TS 36.355 V12.1.0 (2014-03), LTE Positioning Protocol (LPP) (Release 12)